



Engineered Nanoscale Lipid-Based Formulation as Potential Enhancer of Gefitinib Lymphatic Delivery: Cytotoxicity and Apoptotic Studies Against the A549 Cell Line

Abdelrahman Y. Sherif^{1,2} · Gamaleldin I. Harisa^{1,2,3} · Fars K. Alanazi^{1,2} · Fahd A. Nasr⁴ · Ali S. Alqahtani⁴

Received: 23 April 2022 / Accepted: 14 June 2022 / Published online: 1 July 2022
© The Author(s), under exclusive licence to American Association of Pharmaceutical Scientists 2022

Abstract

The present study aimed to engineer a nanoscale lipid-based lymphatic drug delivery system with D- α -Tocopherol polyethylene glycol 1000 succinate to combat the lymphatic metastasis of lung cancer. The nanoscale lipid-based systems including GEF-SLN, GEF-NLC, and GEF-LE were prepared and pharmaceutically characterized. In addition, the most stable formulation (GEF-NLC) was subjected to an in vitro release study. Afterward, the optimized GEF-NLC was engineered with TPGS (GEF-TPGS-NLC) and subjected to in vitro cytotoxicity, and apoptotic studies using the A549 cells line as a surrogate model for lung cancer. The present results revealed that particle size and polydispersity index of freshly prepared formulations were ranging from 198 to 280 nm and 0.106 to 0.240, respectively, with negative zeta potential ranging from -14 to -27.6 mV. An in vitro release study showed that sustained drug release was attained from GEF-NLC containing a high concentration of lipid. In addition, GEF-NLC and GEF-TPGS-NLC showed remarkable entrapment efficiency above 89% and exhibited sustained release profiles. Cytotoxicity showed that IC_{50} of pure GEF was $11.15 \mu\text{g/ml}$ which decreased to $7.05 \mu\text{g/ml}$ for GEF-TPGS-NLC. The apoptotic study revealed that GEF-TPGS-NLC significantly decreased the number of living cells from 67 to 58% when compared with pure GEF. The present results revealed that the nanoscale and lipid composition of the fabricated SLN, NLC, and LE could mediate the lymphatic uptake of GEF to combat the lymphatic tumor metastasis. Particularly, GEF-TPGS-NLC is a promising LDDS to increase the therapeutic outcomes of GEF during the treatment of metastatic lung cancer.

Keywords LDD · Gefitinib · NLC · TPGS · Lung cancer · Cytotoxicity

Introduction

In the first decade of this century, scientists reported that nanoscale particulate systems (20–1000 nm) are transported through the lymphatic system instead of blood capillaries

[70]. Therefore, various nanoscale materials including lipid-based nanoparticles, polymeric micelles, dendrimers, liposomes, polymeric nanoparticles, and others have been developed to achieve lymphatic drug delivery (LDD) [21, 43, 45]. Recently, the nanoscaled lipid-based drug carriers received great attention as lymphatic drug delivery systems (LDDS) due to the inherent lymphatic tropism of these materials in the nanoscale range [21, 38]. During the COVID-19 pandemic, the developed vaccines were loaded into lipid-based formulations to enhance the lymphatic deposition and stimulation of antibody production [38, 44]. In a similar context, LDD could enhance therapeutic outcomes during the treatment of metastatic cancer as a result of the escaping tendency of cancer cells within lymph nodes [53]. Moreover, the escaped cancer cells are considered a red spot for relapse after completing the therapeutic protocol. In this regard, the LDD of anticancer

✉ Abdelrahman Y. Sherif
ashreef@ksu.edu.sa

¹ Kayyali Chair for Pharmaceutical Industry, College of Pharmacy, King Saud University, Riyadh, Saudi Arabia
² Department of Pharmaceutics, College of Pharmacy, King Saud University, Riyadh, Saudi Arabia
³ Department of Biochemistry and Molecular Biology, College of Pharmacy, Al-Azhar University, Nasr City, Cairo, Egypt
⁴ Department of Pharmacognosy, College of Pharmacy, King Saud University, Riyadh, Saudi Arabia

agents ensures the complete elimination of cancerous cells from the body [13].

The nanoscaled lipid-based including solid lipid nanoparticles (SLN), nanostructural lipid carriers (NLC), liquid emulsion (LE), and others were recognized as a carrier for chemotherapeutic agents [2]. These nanoscaled lipid-based formulations are lipoprotein-mimicking nanocarriers to take the same absorption track through the lymphatic system [14]. The major difference between SLN, LE, and NLC is the composition of the lipid core which consist of solid lipid, liquid oil, and mixed solid and liquid oil, respectively [2]. These nanoscale lipid-based systems are biodegradable, biocompatible, and feasible for large-scale production [2]. Moreover, the accumulation of nanoscale drug cargo into tumor tissue is greater than normal due to poor lymphatic drainage and the enhanced permeability and retention effect [34, 61].

Interestingly, the engineering of nanoscaled lipid-based formulation plays a crucial role in the therapeutic outcomes [8]. This resulted from enhanced drug distribution to its site of action with reduced systemic toxicity [20]. For example, coating nanoparticles with polyethylene glycol (PEG) allow them to evade opsonization and phagocytosis by macrophages. This increases the circulation time of the drug that is loaded within nanoparticles and increases the chance of distribution to the lymphatic system and tumor mass [23]. In addition, caveolin and clathrin receptors are highly expressed on the surface of cancerous cells [65]. Therefore, negatively charged nanoparticles are susceptible to cancer delivery through caveolin and clathrin-mediated endocytosis [32]. Furthermore, it was reported that vitamin E-coated nanoparticles are more susceptible to uptake through receptor-mediated endocytosis that overexpressed on cancerous cells [29]. In addition, the biodistribution study showed that drug-loaded lipid-based nanoparticles consisting of stearic acid were highly distributed to lung cells [64]. Collectively, engineering nanoscale lipid-based formulation enhances the LDD of administered chemotherapeutic agents. Further studies are required to confirm this topic.

GEF inhibits cell proliferation by blocking epidermal growth factor receptor signaling. It is approved by FDA for the treatment of non-small lung cancer [28]. Moreover, various researches showed that GEF has cytotoxic activity against hepatocellular carcinoma [48], colorectal cancer [30], and breast cancer [36]. Furthermore, GEF exhibits antiviral activity against various types of viruses including SARS-Cov-2 [6, 26]. Many studies suggested that the nanoscale drug delivery system could improve the therapeutic outcomes of GEF [17, 54]. However, further studies are still required to develop a GEF-loaded nanoscale lipid-based formulation as LDDS.

Therefore, the present study aimed to engineer D- α -Tocopherol polyethylene glycol 1000 succinate (TPGS) nanoscale gefitinib-loaded lipid-based as LDDS of GEF to combat the lymphatic metastasis of lung cancer. GEF solid lipid nanoparticles (GEF-SLN), GEF nanostructured lipid carriers (GEF-NLC), and GEF liquid emulsion (GEF-LE) were prepared and subjected to pharmaceutical characterization. The best lipid-based nanoparticles were subjected to *in vitro* dissolution to select the optimum formulation. In addition, stability was studied to select the more stable nanoscale lipid-based carrier. Finally, the optimized formulation NLC was engineered with TPGS (GEF-TPGS-NLC) and subjected to cytotoxicity and apoptotic studies against the A549 cells line as surrogate model none small lung cancer.

Materials and Methods

Materials

Gefitinib (GEF) was purchased from Beijing Mesochem Technology Co. Ltd. (Beijing, China). Pluronic-F68 (PF-68) and D- α -Tocopherol polyethylene glycol 1000 succinate (TPGS) were purchased from Sigma Aldrich, St. Louis, MO, USA. Stearic acid (SA) was purchased from BDH, Poole, UK. Oleic acid (OA) was obtained from Avonchem, Cheshire, UK.

Preparation of SLN, NLC, and LE

Lipid-based formulations were prepared as previously described [19] using the ultrasonic melt-emulsification method with minor modification. Each formulation was prepared as described in Table 1. Briefly, an aqueous phase was prepared by mixing the predetermined amount of surfactant and TPGS (in the case of TPGS-NLC) in distilled water. The lipid phase was prepared by adding the weighted amount of lipid without (Plain-SLN or Plain-NLC or Plain-LE) or with GEF (GEF-SLN or GEF-NLC or GEF-LE) in a cylindrical beaker. During preparation, both beakers are heated up to 80 °C simultaneously. The beaker containing liquefied lipid was placed above preheated Magnetic-Stirrer heater at 80 °C then the hot aqueous phase was added gradually. The magnetic stir was added then the mixing speed was increased up to 5000 rpm for 3–5 min to obtain the primary microemulsion. After that, the lipid-based formulation was obtained using probe-sonication at 80% voltage efficiency for 3 min (10 s/cycle followed by resting period of 5 s). The obtained lipid-based formulation was placed immediately in the refrigerator till cooling.

Physicochemical Characterization

Particle Size, Polydispersity Index, and Zeta Potential

Particle size (PS), polydispersity index (PDI), and zeta potential (ZP) for each formulation was measured using a Zetasizer Nano ZS (Malvern Instruments, UK). Each formulation was diluted (1: 1000) in distilled water and evaluated at 25 °C. (Particle size beside PDI) and ZP were measured using dynamic light scattering and laser doppler velocimetry mode, respectively. The found values were taken as an average of three measurements where each value was reported as an average of six measurements [19].

Differential Scanning Calorimetry

GEF, SA, SA: OA (3:1), PF-68, GEF-SLN_{1,3} and GEF-NLC_{1,3} were subjected to differential scanning calorimetry (DSC) analysis using the DSC – 8000 Perkins Elmer (Waltham, MA, USA) apparatus in a temperature range of 25–250 °C at heating rates of 10 °C/ min. The samples were evaluated with the purge of nitrogen at around 20 mL/ min, and an autosampler and a chiller were installed on this apparatus. The weight of each sample was 3 mg and fixed inside the sealed aluminum pan. For the characterization and evaluation of the samples, a Pyris manager software (Pyris Elmer, Waltham, MA, USA) was used for the solid-state characterization [4].

Powder X-ray Diffraction

The powder X-ray diffraction (PXRD) spectra of the GEF, SA, freshly melted and cooled SA, PF-68, GEF-SLN_{1,3} and GEF-NLC_{1,3} were performed to evaluate the molecular state of SA and GEF crystallinity after preparing lipid-based formulation. The study was conducted using an X-ray diffractometer (Ultima IV, Rigaku Inc. Tokyo, Japan) with a scanning rate of 0.5/min in the scanning range of 3–180°. The characteristic peak of each sample was assessed by collecting the data by monochromatic radiation (Cu Kα¹, λ = 1.54 Å), operating at a voltage of 40 kV and current of 40 mA [4].

Encapsulation Efficiency

The encapsulation efficiency (EE%) of the GEF in drug-loaded NLC was measured by the indirect method. Briefly, a predetermined amount from the prepared formulation was centrifuged for 30 min at 50,000 rpm to precipitate loaded NLC. The amount of the drug in the supernatant was measured using the developed UV-UPLC method. EE% was determined using the following equation [5, 41]:

Table 1 Composition of the Prepared Plain-SLN, GEF-SLN, Plain-NLC, GEF-NLC, GEF-TPGS-NLC, Plain-LE, and GEF-LE

Formulation code	Lipid phase		Aqueous phase		Drug GEF
	SA	OA	PF-68	TPGS	
Plain-SLN ₁	600		200		
Plain-SLN ₂	800		200		
Plain-SLN ₃	1000		200		
GEF-SLN ₁	600		200		40
GEF-SLN ₂	800		200		40
GEF-SLN ₃	1000		200		40
Plain-NLC ₁	450	150	200		
Plain-NLC ₂	600	200	200		
Plain-NLC ₃	750	250	200		
GEF-NLC ₁	450	150	200		40
GEF-NLC ₂	600	200	200		40
GEF-NLC ₃	750	250	200		40
GEF-TPGS-NLC	750	250	200	20	40
Plain-LE ₁		600	200		
Plain-LE ₂		800	200		
Plain-LE ₃		1000	200		
GEF-LE ₁		600	200		40
GEF-LE ₂		800	200		40
GEF-LE ₃		1000	200		40

The amount was expressed in mg units. The predetermined amount of surfactant was dissolved in 20 g of distilled water as a continuous phase in all formulations. *Plain-SLN* drug free-solid lipid nanoparticle, *GEF-SLN* gefitinib-loaded solid lipid nanoparticle, *Plain-NLC* drug free-nanostructural lipid carrier, *GEF-NLC* gefitinib-loaded-nanostructural lipid carrier, *GEF-TPGS-NLC* gefitinib-loaded PEGylated nanostructural lipid carrier, *Plain-LE* drug free-liquid emulsion, *GEF-LE* gefitinib-loaded- liquid emulsion, *SA* stearic acid, *OA* oleic acid, *PF-68* Pluronic F-68, *TPGS* D-α-Tocopherol polyethylene glycol 1000 succinate

$$EE\% = \frac{\text{Total amount of GEF (mg)} - \text{Amount of GEF in supernatant (mg)}}{\text{The total amount of GEF (mg)}}$$

* 100

Stability of Prepared Formulations

The prepared lipid-based formulations were put within a 20-ml glass vial and placed in a refrigerator at 4 °C. The stored formulations were characterized in terms of PS, PDI, and ZP for 3 months.

In Vitro Dissolution

In vitro release of GEF was performed using a previously described dialysis method with minor modification [54]. An amount equivalent to drug suspension or formulation containing 0.5 mg of GEF diluted (1:4) in phosphate buffer was placed inside a dialysis membrane bag (molecular weight

cut off: 12–14 kDa) and sealed. This bag was placed in a beaker containing a preheated 100 ml medium of simulated intestinal fluid (pH 6.8) containing 0.5% T-80. The beaker was continuously shaken at 100 rpm at 37 ± 1 °C in a thermostat shaker. Samples were withdrawn at 5, 10, 15, 30, 30, 60, 120, 240, 480, 720, 960, and 1440 min and an equal amount of dissolution media was replaced. The withdrawn samples were centrifuged for 10 min at 10,000 rpm and the amount of drug in the supernatant was determined using the developed UV-UPLC method.

Cell Culture

Human non-small-cell lung carcinoma (NSCLC) cell lines (A549) were obtained from DSMZ Leibniz Institute (German Collection of Microorganisms and Cell Cultures Braunschweig, Germany). Cells were maintained in the incubator at 37 °C in a humidified incubator with 5% CO₂, in DMEM culture medium, supplemented with 10%v/v FBS (Gibco; USA) and 1%v/v penicillin–streptomycin.

In Vitro Cytotoxicity

The cytotoxic evaluation of the selected formulations against A549 cell lines was performed by MTT assay as previously described by [35]. Briefly, cells were plated at 1×10^5 cells per well in 96-well for 24 h. Thereafter, the cells were treated with different concentrations (2.5–20 µg/ml) of pure GEF (dissolved in DMSO), Plain-TPGS-NLC, and drug-loaded formulations (GEF-NLC, and GEF-TPGS-NLC). After 48 h of incubation, 10 µl of MTT solution (5 mg/ml) was added to each well and further incubated in the dark for 4 h at 37 °C. Next, the formazan product was solubilized with acidified isopropanol and the absorbance was measured at a wavelength of 570 nm using a microplate reader (Bio-Tek, USA). The dose–response curves were used to calculate the IC₅₀ (concentration required to inhibit cell growth by 50%). Cell viability was calculated according to the following equation:

$$\text{Cell viability (\%)} = (\text{optical density of the treated sample}) / (\text{optical density of the untreated sample}) \times 100\%$$

Flow Cytometric Analysis of Cells Apoptosis

Flow cytometric analysis was employed to quantify cell apoptosis using an Annexin-V/FITC/PI staining Kit (Sigma, USA) according to the manufacturer's instructions. In brief, A549 cells were seeded in a 12-well plate at a density of 1×10^5 cells/well, and after overnight incubation, cells were treated with IC₅₀ of pure GEF (3.5 µg/ml; calculated from current in vitro cytotoxicity study) as well as the equivalent concentration of PLAIN-SLN and GEF-C-CSLN. After 48 h of incubation, treated and untreated cells were collected, washed with cold PBS (1x), and resuspended in 100 µL of

binding buffer (1x) with FITC Annexin V (5 µL) and PI (5 µL). After 20 min incubation in the dark, 400 µL of binding buffer was added and the samples were analyzed by flow cytometry (Cytomics FC 500; Beckman Coulter, Brea, CA, USA) [35].

Statistical Analysis

The data were statistically evaluated using SPSS software, Version 26. The results were compared using an independent *t*-test (for data with two sets). Data were expressed as mean \pm SD. *P*-value < 0.05 was used as the criterion for significance.

Results and Discussion

Physicochemical Properties of SLN, NLC, and LE

The particle size of Plain (blue color) and GEF-loaded (orange color) SLN, NLC, and LE formulations are shown in Fig. 1 (A, B, and C). Generally, the increase in the particle size following increasing lipid content could be attributed to a decreased ratio of surfactant: total lipid used during the production of lipid-based nanoparticles. The obtained results are in alignment with the observation reported during the production of different lipid-based nanoparticles [24, 31, 47]. Moreover, Plain lipid-based nanoparticles had a smaller particle size compared to corresponding GEF-loaded lipid-based nanoparticles. The observed increase in the particle size of lipid-based nanoparticles following the incorporation of GEF could attribute to the increased content of the lipid core. This is in alignment with various studies that showed that Plain lipid-based nanoparticles were smaller than corresponding drug-loaded SLN [40, 60], NLC [18, 50], and LE [1, 16]. In contrast to high lipid concentration (4.72%), the particle size of lipid-based nanoparticles at each concentration was arranged as follows: Plain-LE < GEF-LE < Plain-NLC < GEF-NLC < Plain-SLN < GEF-SLN. The reduction in particle size of SLN after partial or complete replacement of solid lipid with liquid oil in NLC or LE, respectively, could be attributed to a reduction in the viscosity of lipid core during sonication. Herein, the measured melting point of SA, SA: OA (3:1), and OA is 71.1, 53.8, and 13 °C, respectively. Therefore, it is expected to obtain higher viscosity of media during the production of SLN. In this context, Zardini et al. stated that using lipid with a low melting point resulted in the production of smaller particles [68]. Moreover, a linear relationship between the concentration of lipid and particle size of Plain or GEF-loaded lipid-based formulation was observed with exception of GEF-SLN formulations. This could be attributed to a pronounced disruption in SA crystallinity in GEF-SLN₁ which contain a high

drug: lipid ratio. On contrary, GEF-SLN₃ showed a smaller particle size even with the presence of a high concentration of lipid. This is attributed to the presence of GEF in low drug: lipid ratio in GEF-SLN₃ where its effect is very diluted. This allowed the packing of SA in the SLN core in minimal space. This observation by Dantas et al. stated that the presence of the lipophilic drug in beeswax (solid lipid) resulted in a loss of lipid crystallinity [12].

PDI values of SLN, NLC, and LE formulations are shown in Fig. 1 (D, E, and F). An analogous trend was observed with Plain (blue color) and GEF-loaded (orange color) SLN, and LE formulations. The importance of PDI value from its reflection on the homogenous distribution of nanoparticles in the prepared formulation. This ensures the stability of formulation and reproducibility of therapeutic outcomes [10, 67]. Therefore, nanoformulations with PDI values less than 0.3 are considered homogenous [57]. Herein, the prepared lipid-based nanoformulations were homogeneously distributed in the measured nano-size range with a PDI value of less than 0.3.

Zeta potential values of Plain (blue color) and GEF-loaded (orange color) SLN, NLC, and LE are shown in Fig. 1 (G, H, and I). Zeta potential value for nanoparticles is an important factor during the expectation of formulation stability. Therefore, increasing the zeta potential value either on the negative or positive side is expected to enhance stability and prevent particle aggregation as a result of the repulsion effect [68]. Additionally, negative nanoparticles are less susceptible to the opsonization process which extent their circulation time [33]. The prepared formulations had a negative zeta potential value which is expected to enhance stability and therapeutic outcome.

DSC

DSC graph of GEF, PF-68, freshly melted then cooled SA, GEF-SLN₁, and GEF-SLN₃ are shown in Fig. 2, A. Moreover, Fig. 2 B shows the DSC graph of GEF, PF-68, freshly melted then cooled SA: SA (3:1), GEF-NLC₁, and GEF-NLC₃. The detected melting point of GEF and PF-68 was 195.7 and 53.8 °C, respectively, that almost equivalent to

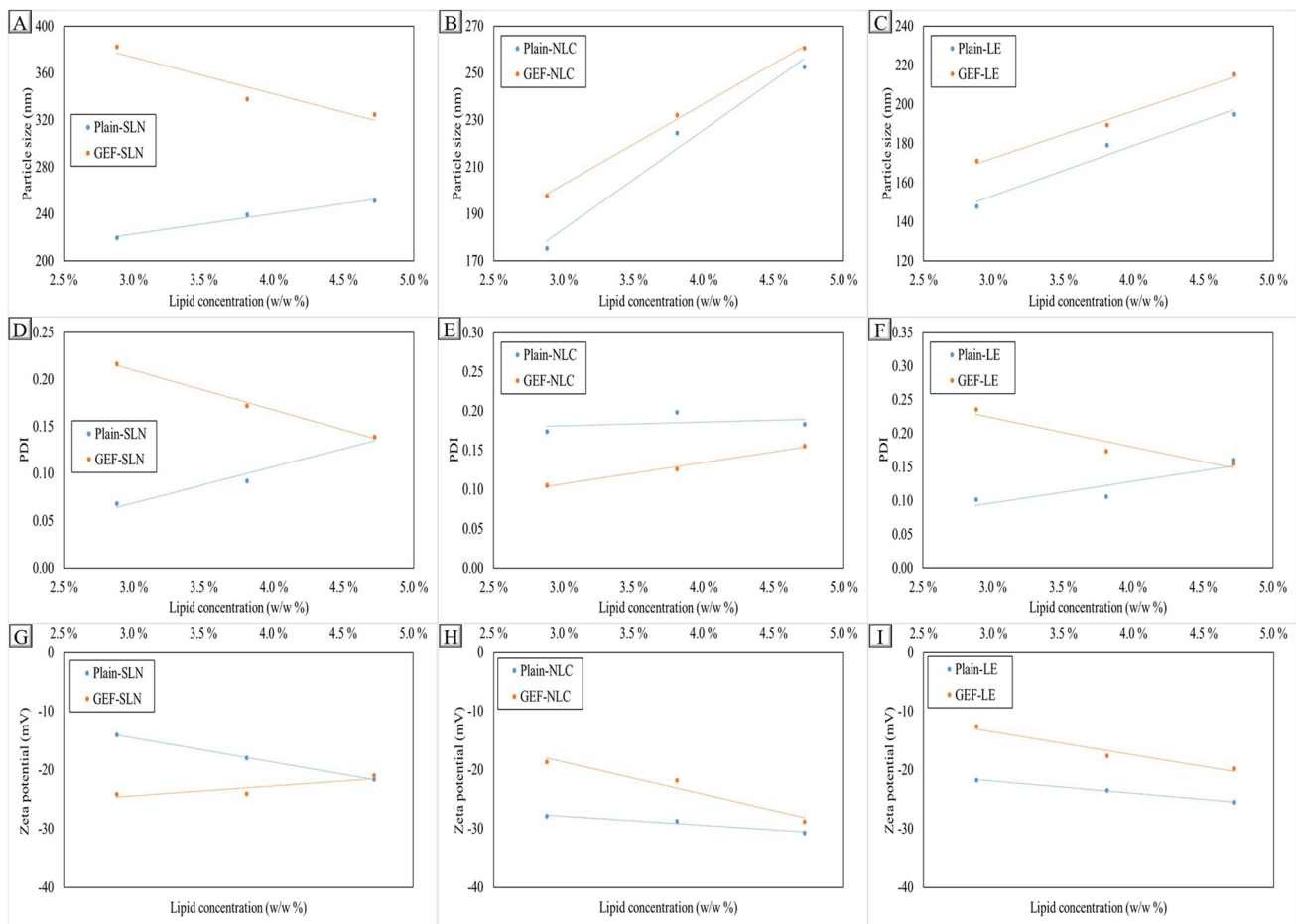


Fig. 1 A, B, C Particle size, D, E, F PDI, and G, H, I zeta potential values of prepared both drug-free and drug-loaded SLN, NLC, and LE

previously reported [4, 15]. The DSC scanning for freshly melted then cooled SA and SA: SA (3:1) was performed to observe the influence of the process on the melting point. The observed melting point was 71.1 and 65.3 °C, respectively. The slight shifting and broadening of the SA peak could be attributed to the presence of OA which reduce the melting point and crystallinity of SA, respectively. This agreed with Yang et al. who stated that the presence of different types of liquid oils reduced the melting point of solid lipid [66].

The melting points of GEF-SLN formulations were almost equal to the melting point of SA. It was 69.4 and 70.1 °C for SLN₁, and GEF-SLN₃ formulations, respectively. A similar observation was obtained with GEF-NLC formulations where the melting point of GEF-NLC₁ and GEF-NLC₃ were 64.4 and 66.4 °C, respectively. However, both GEF-SLN and GEF-NLC did not show a melting point for GEF that indicate either the homogenous distribution of GEF in the lipid core or the presence of the drug in the amorphous state. In agreement with the obtained results, different researchers showed that the incorporation of the lipophilic drug in SLN [3, 52] and NLC [46, 55] resulted in the disappearance of the drug peak. This confirmed presence of the drug in an amorphous state or homogenous distribution in the lipid phase.

PXRD

The crystalline diffraction patterns of GEF, freshly melted and cooled SA, GEF-SLN₁, and GEF-SLN₃ are shown in Fig. 3, A. Moreover, Fig. 3 B shows the DSC graph of GEF, freshly melted and cooled SA: SA (3:1), GEF-NLC₁, and GEF-NLC₃. PXRD graph of GEF shows high-intensity peaks at 38.1° and 44.3° in addition to multiple peaks with moderate intensity at 19.4, 24.2, 26.4°, and 77.5°. Furthermore, freshly melted, and cooled SA showed high-intensity diffraction peaks at 6.7, 11.1, 21.7, 24.3, 38.1, and 44.3°. The diffraction pattern of freshly melted and cooled SA: SA (3:1) was different from SA in a reduction in peaks at 21.7, 24.3, 38.1, and 44.3°. Finally, the PXRD pattern of GEF-SLN and GEF-NLC formulations shows a pronounced reduction in 6.7, and 11.1 peaks with the disappearance of two predominant peaks of SA and GEF at 38.1° and 44.3°.

The diffraction pattern of SA showed multiple peaks with high intensity that reflected a high degree of crystallinity. Moreover, the reduction in SA crystallinity after the incorporation of OA is attributed to the fluidization effect produced by liquid oil. Furthermore, PXRD was performed for formulations containing the highest and lowest solid lipid: drug ratio. PXRD pattern showed the disappearance of the predominant peak of GEF indicating the presence of the drug in an amorphous state. Moreover, the reduction in SA peaks could be attributed

to the disorientation of crystals packing in presence of GEF. In agreement with the obtained results, Pawar et al. found that the presence of GEF in the lipid matrix of SA resulted in a significant reduction in its crystallinity [42]. In addition, Dantas et al. found that the presence of the lipophilic drug in SLN resulted in a significant reduction in lipid crystallinity [12]. Regarding NLC, Li et al. found that the incorporation of the lipophilic drug in NLC resulted in a significant reduction in drug crystallinity [27]. Taken all these together, the incorporation of lipophilic drugs in the lipid core during the production of lipid-based nanoparticles resulted in a significant reduction in drug crystallinity.

Stability of Prepared Formulations

Physicochemical properties of GEF-NLC formulations during the stability study are shown in Fig. 4. All formulations were stored in a refrigerator for 3 months and they were subjected to physicochemical characterization for the stability study. Both Plain-LE and GEF-LE formulations showed gelling formulation after 1–2 days of storage. Even though Plain-SLN showed a high degree of stability, GEF-SLN was unstable and particle aggregation was observed after 3 months. This could be attributed to the expulsion of the drug from the lipid core towards the nanoparticle coat. This resulted in a significant alteration in surface properties and particle aggregation was detected. Therefore, aggregated particles at bottom of the bottle from the high and low drug: lipid ratio (GEF-SLN₁ and GEF-SLN₃, respectively) were collected. They were subjected to DSC and PXRD characterization as shown in Fig. 5 (A and B, respectively). Thermo-scanning showed additional endothermic peaks between 90 and 140 °C which could be attributed to GEF. These peaks are more pronounced in the case of GEF-SLN₁ precipitate than GEF-SLN₃. Moreover, PXRD for aggregated particles showed the appearance of crystalline peaks of GEF. In addition, PXRD shows peaks at 38.1 and 44.3° and it is also more pronounced in the case of GEF-SLN₁ precipitate. Taken all these together, explain of GEF from core to coated resulted in particle aggregation.

Regarding GEF-NLC, the prepared formulations were stable, and no particle aggregation was not observed. This could be attributed to the solubilization of GEF in liquid oil (oleic acid). Therefore, using liquid oil beside solid lipid ensures formulation stability. However, the instability of GEF-LE could be attributed to the presence of oleic acid in a higher amount that alters the surface properties of nanoparticles. This could be the reason for instability and observed particle aggregation. Table 2 summarizes the physicochemical properties and stability of prepared lipid-based nanoparticles (SLN, NLC, and LE).

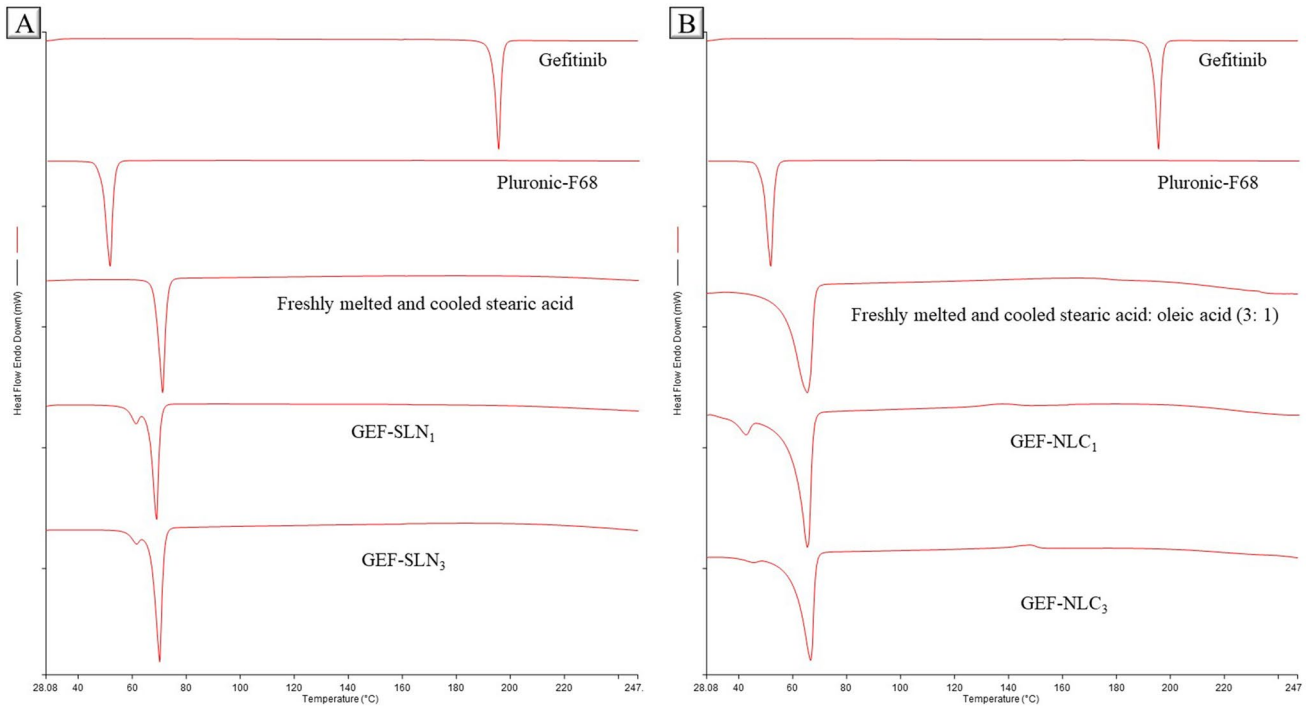


Fig. 2 GEF, PF-68, freshly melted and cooled SA, GEF-SLN₁, GEF-SLN₃, freshly melted and cooled SA: SA (3:1), GEF-NLC₁, and GEF-NLC₃

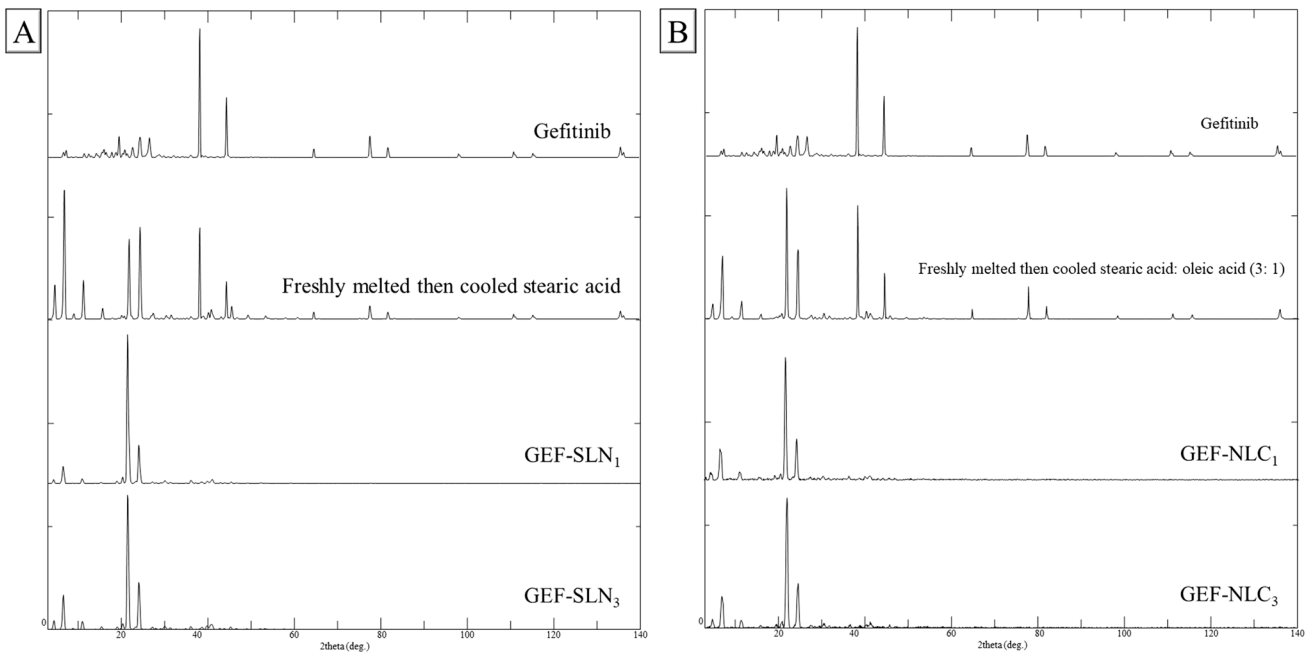


Fig. 3 PXRD of GEF, freshly melted and cooled SA, GEF-SLN₁, GEF-SLN₃, freshly melted and cooled SA: SA (3:1), GEF-NLC₁, and GEF-NLC₃

Physicochemical Properties of GEF-TPGS-NLC Formulation

The impact of TPGS on the physicochemical properties of GEF-NLC is shown in Fig. 6. The particle size of GEF-NLC was increased from 260.6 to 288.1 nm after the incorporation of TPGS. Furthermore, the zeta potential value was increased from -28.8 to -26.5 with no significant difference. Finally, both formulations showed a remarkable entrapment efficiency (above 92%) was no significant difference between both formulations.

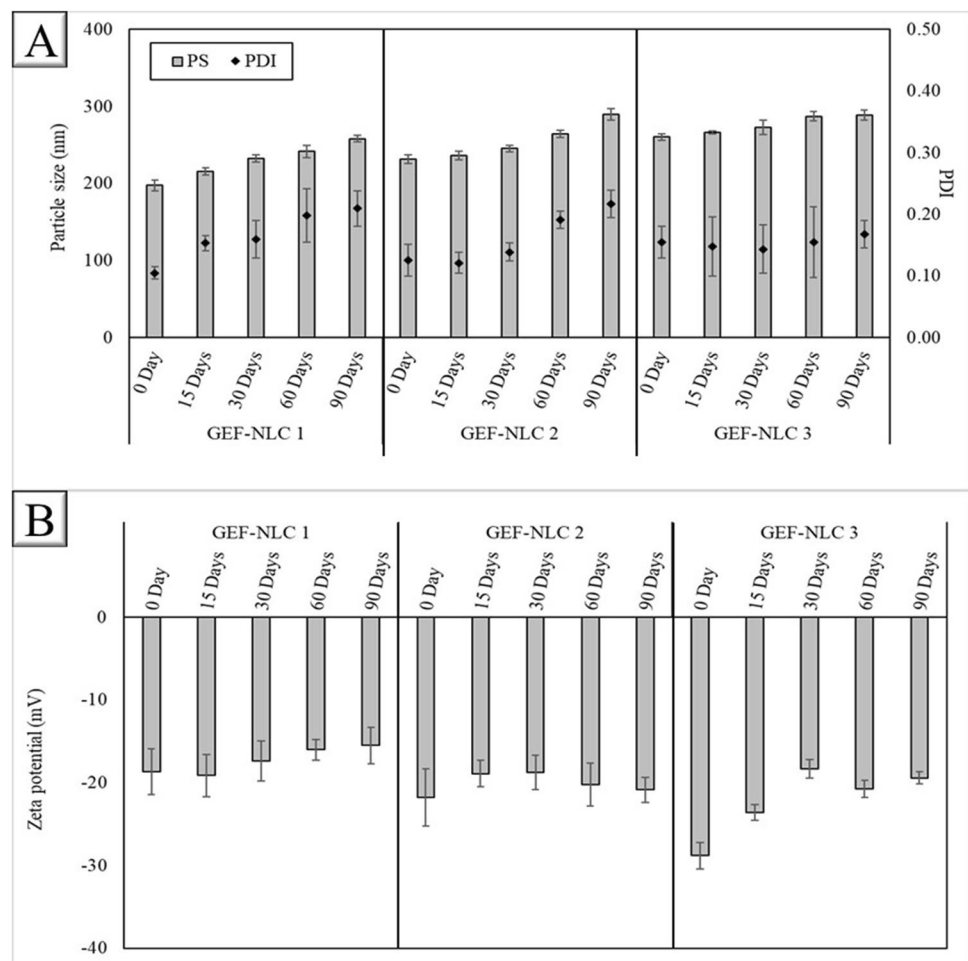
The enlargement in the NLC size could be attributed to the coating effect produced by the PEG portion of TPGS. In alignment with the obtained results, Banerjee et al. found that particle size and PDI of drug-loaded NLC were increased after the incorporation of TPGS [7]. Likewise, Zhao et al. found that TPGS-free NLC was smaller and more homogenous when compared with coated NLC [72]. In addition, the incorporation of TPGS did not produce a significant difference in EE of loaded drugs. On contrary, Banerjee et al. stated that the incorporation of TPGS led to a decrease in the zeta potential value of prepared lipid-based nanoparticles [7].

In Vitro Release

The dissolution profile of GEF-NLC₁, GEF-NLC₂, GEF-NLC₃, and GEF-TPGS-NLC is shown in Fig. 7. It is clear from the figure that all formulations showed burst drug release up to 2 h and follow zero-order behavior. Moreover, sustained drug release was observed until 8–12 h with no notable drug release until the end of the experiment. Comparing GEF-NLC formulation, GEF-NLC₁ exhibited faster drug release compared to the other formulations. This could be attributed to the solubilization of the drug within a minimal amount of lipid compared to other formulations. Therefore, the residence of the drug within lipid nanoparticles until permeation through the intestinal membrane ensures lymphatic delivery of the administered therapeutic agent. GEF-NLC₃ was selected as the optimum formulation and subjected to a dissolution study to study the effect of TPGS on drug release. It is clear from the figure that TPGS did not show any significant difference in drug release.

In harmony with the obtained results, Banerjee et al found that TPGS coated GEF-NLC produces more

Fig. 4 **A** Particle size, PDI, and **B** zeta potential values of GEF-NLC formulations



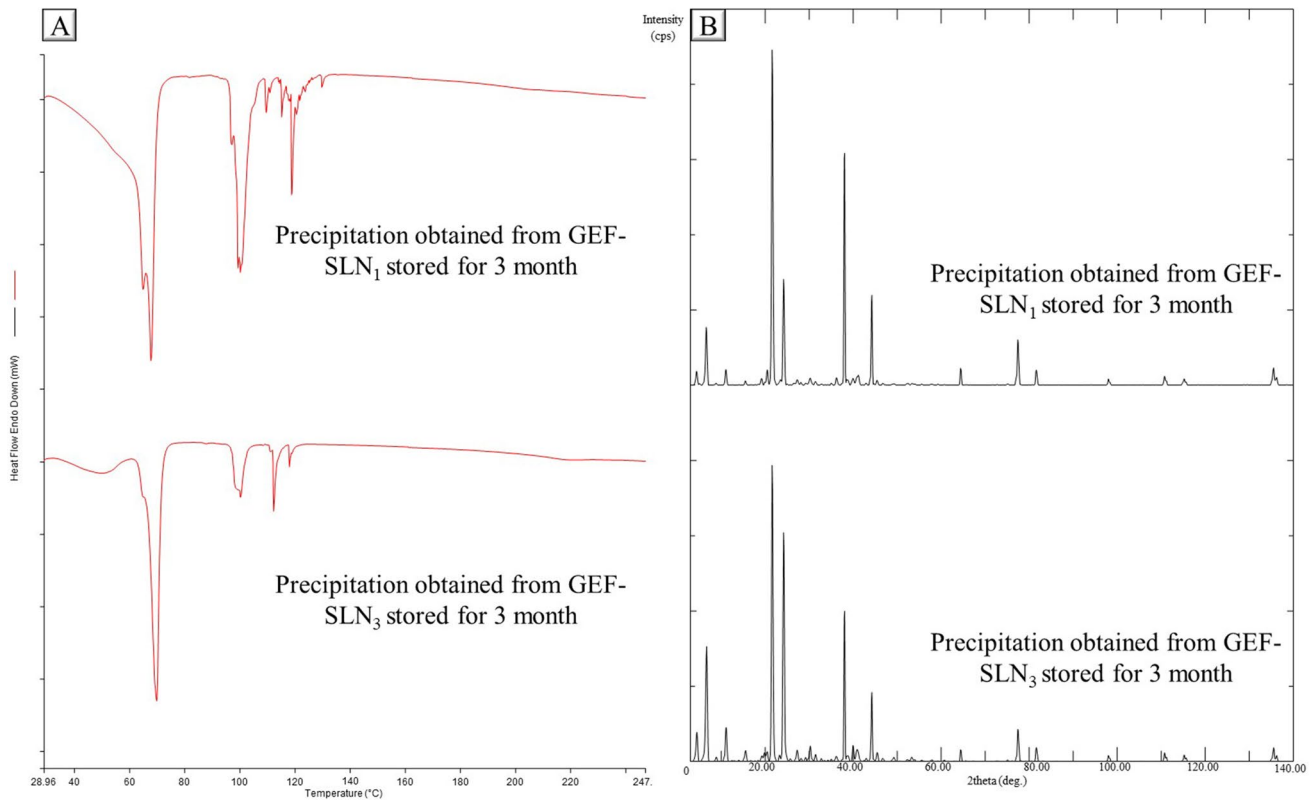


Fig. 5 **A** DSC and **B** PXRD of GEF-SLN formulations

sustained drug release compared to uncoated NLC which could be attributed to the increased thickness of the diffusion layer [7]. Additionally, Zhao et al. found that loaded drug was faster released from unmodified NLC compared to TPGS coated NLC [72]. In addition, Vaidya et al found that PEGylated SLN showed a slower drug release compared to un-PEGylated one [59]. However, Cho et al. developed two lipid-based formulations coated either with TPGS or Tween-80. The in vitro dissolution study showed that both formulations exhibit similar release patterns with no significant difference [9].

In Vitro Cytotoxicity

The nanoscale pharmaceutical formulations are postulated to enhance the cytotoxicity of chemotherapeutic agents. In this study, the optimized GEF-NLC₃ and GEF-TPGS-NLC were selected to achieve the in vitro cytotoxicity study due to their ability to retain the drug and this might increase their susceptibility to lymphatic delivery. The inhibitory effects of pure GEF, Plain-TPGS-NLC, GEF-NLC, and GEF-TPGS-NLC on the growth of A549 cells were studied using an MTT assay. Figure 8 (A and B) showed the effect

Table 2 Physicochemical Properties and Stability of the Prepared Nanoscale Lipid-Based Nanoparticles

Formulation type	SLN		NLC		LE	
	Plain-SLN	GEF-SLN	Plain-NLC	GEF-NLC	Plain-LE	GEF-LE
Lipid core composition	Solid lipid		Solid lipid beside liquid oil		Liquid oil	
Particle size	220—252	383 – 325	175 -253	198 – 261	148—195	172 – 215
PDI	0.068—0.139	0.139 – 0.217	0.174 – 0.198	0.105 – 0.155	0.102 – 0.160	0.155 – 0.236
Zeta potential	(-22) – (-14)	(24-) – (-21)	(-31) – (-28)	(-29) – (-19)	(-26) – (-22)	(-20) – (-13)
Stability	Stable for 3 months	Stable for 1 month	Stable for 3 months		Unstable for more than 1—2 days	
Decision	—	Excluded	—	Selected	—	Excluded

of formulations at four different concentrations (2.5, 5, 10, and 20 $\mu\text{g/ml}$) on the cell viability following 24 and 48 h incubation time. Regarding Plain-TPGS-NLC, an equivalent volume similar to GEF-TPGS-NLC at each concentration was incubated to study the toxicity of drug-free formulation. All formulations inhibited the growth of A549 cells in a concentration-dependent manner. The results revealed that more than 75% of the cell were able to survive following incubation for 24 h with Plain-TPGS-NLC at a higher concentration (20.0 $\mu\text{g/ml}$). In addition, Plain-TPGS-NLC showed a significantly lower cytotoxic activity following incubation for 48 h compared with other formulations. Moreover, GEF-TPGS-NLC was able to produce a significant cytotoxic activity at all concentrations except 20 $\mu\text{g/ml}$ following incubation for 24 h. However, there is no significant difference in cytotoxic activity between GEF-TPGS-NLC, Pure GEF, and

GEF-NLC following 48 h incubation. Furthermore, Table 3 showed the IC_{50} for Pure GEF, GEF-NLC, and GEF-TPGS-NLC at 24 and 48 h. IC_{50} following 24 h incubation for pure GEF, GEF-NLC, and GEF-TPGS-NLC was 11.16, 15.05, and 7.01 $\mu\text{g/ml}$, respectively. However, IC_{50} of pure GEF, GEF-NLC, and GEF-TPGS-NLC decreased to 3.54, 4.35, and 3.60 $\mu\text{g/ml}$, respectively, following 48 h incubation. It should be noted that IC_{50} for Plain-TPGS-NLC cannot calculate at both incubation times.

It was found that GEF-TPGS-NLC was able to produce significant cytotoxic activity compared to pure GEF. However, Pure GEF was able to produce pronounced cytotoxic activity compared to the GEF-NLC formulation. This could be attributed to the properties of surfactants used during the production of drug-loaded NLC. Pluronic is tri-block polymers composed of hydrophobic polypropylene oxide attached from both sides to hydrophilic polyethylene oxide [69]. Therefore, it is expected to align the hydrophilic polypropylene oxide outside NLC to form a coat. This will prevent the binding and internalization of nanoparticles inside cells [11]. This is following Tsai et al. findings which developed polypropylene glycol coated nanoparticles that exhibited low cellular internalization. This could attribute to the shielding effect produced by hydrophilic coat [58]. The cytotoxic activity of GEF-TPGS-NLC could be attributed to the presence of TPGS. TPGS is a nonionic surfactant consisting of PEG polymer covalently connected to vitamin E. The former reduces particle clearance while the latter enhances permeation and uptake through vitamin E receptors [29]. In this context, Tsai et al. found that TPGS-coated nanoparticles showed a high internalization compared to PEG-coated nanoparticles which attributed to the presence of efflux transporter inhibitors [58]. On the other hand, cytotoxicity for studied formulations following 48 h incubation

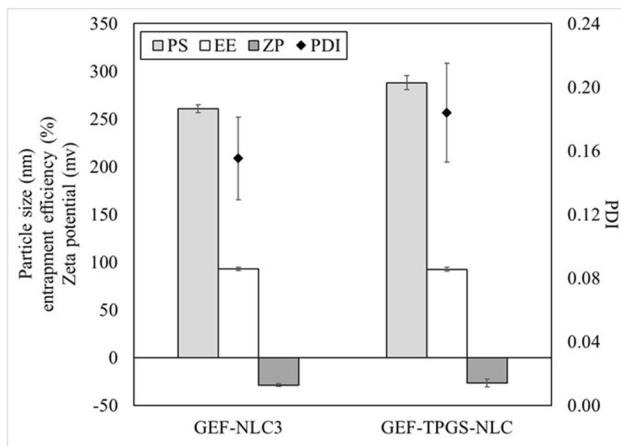


Fig. 6 Particle size, PDI, zeta potential, and entrapment efficiency of GEF-NLC and GEFTPGS-NLC

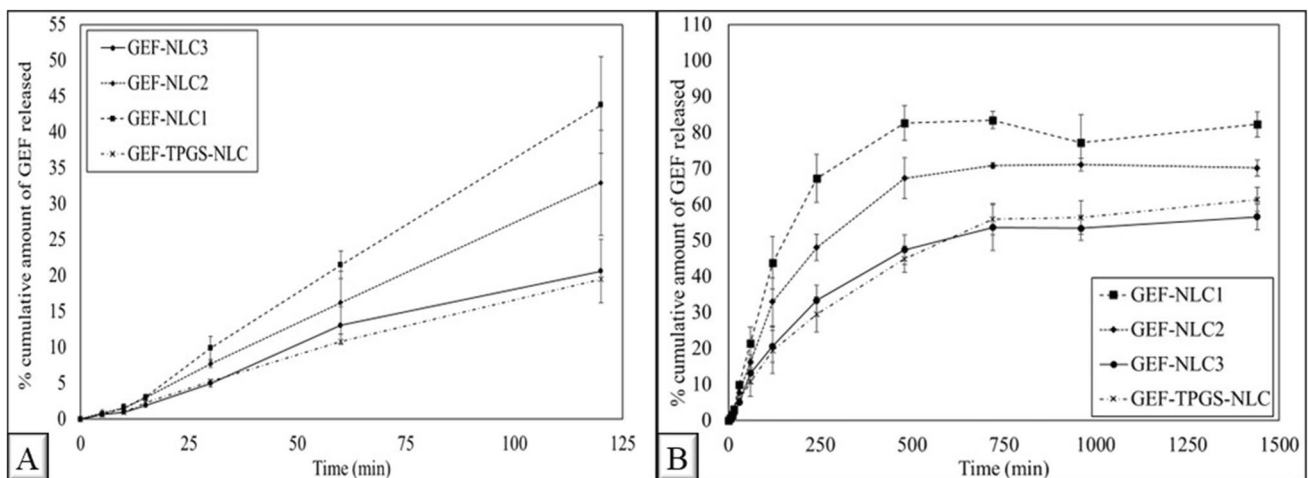


Fig. 7 In vitro release profile of GEF-NLC1-3 and GEF-TPGS-NLC in phosphate buffer containing 0.5% T-80. Data were expressed as the mean \pm SD, $N=3$

did not show any significant difference. This could be attributed to the incubation of the tested formulations' insufficient time to produce cytotoxic activity.

The obtained results agreed with Zhang et al. who studied cellular uptake of drug-loaded NLC and polymeric nanoparticles. The results revealed that NLC was able to enhance cellular uptake more than polymeric nanoparticles which could be attributed to adherence tendency to lipid surface [71]. Furthermore, Banerjee et al. found that free cytotoxic drug and drug-loaded NLC had high IC₅₀ than drug-loaded TPGS-NLC. Moreover, a cellular uptake study was performed using a confocal microscope and drug-loaded TPGS-NLC produces higher intensity than drug-loaded NLC. The authors refer to this as the solubilization and penetration enhancement effect produced by the PEG portion of TPGS. In addition, TPGS inhibits efflux transporter with increasing accumulation of drugs inside cancer cells [7]. Likewise, Shirazi et al. found that incorporation of TPGS within NLC formulation reduces IC₅₀ of a cytotoxic agent by fourfold compared to drug solution [51]. It was found that drug-loaded SLN was more cytotoxic compared to a pure drug following 24 h incubation. However, there was no significant difference between pure drug and drug-loaded NLC after 48 and 72 h incubation [60]. The incorporation of the cytotoxic agent within smaller nanoparticles enhances cellular internalization and escaped efficiently from phagocytosis [25].

Apoptotic Study

Elimination and removal of unwanted cells are ensured through a complex physiological process known as apoptosis. Therefore, this study is conducted to sort and quantify the cells' population following their treatment with chemotherapeutic agents [62]. Annexin V/PI double staining was utilized in the current study to stain A549 cells treatment with pure GEF, Plain-TPGS-NLC, GEF-NLC, and

GEF-TPGS-NLC for 24 h. The incubation time was selected to observe the difference between pure GEF and GEF-TPGS-NLC based on the MTT assay. The cells were treated with 11.15 µg/ml from all formulations that were equivalent to IC₅₀ of pure GEF. As shown in Fig. 9, pure GEF exposure at 11.15 µg/ml concentration led to an increase in early apoptotic, late apoptotic, and necrotic cells population (11.17 ± 2.25, 12.97 ± 2.98, and 5.90 ± 1.48%, respectively) compared to untreated cells (2.40 ± 1.30, 3.57 ± 0.25, and 4.33 ± 0.96%, respectively). Interestingly, there are a significant reduction in cell viability from 69.9 ± 3.5 to 58.4 ± 2.2% after cell treatment with pure GEF and GEF-TPGS-SLN, respectively. Moreover, the early apoptotic, late apoptotic, and necrotic cells population following treatment with GEF-TPGS-NLC were 9.7 ± 1.0, 12.4 ± 1.4, and 19.5 ± 0.6%, respectively.

Practically, conventional administration of GEF resulted in poor therapeutic outcomes when used at lower concentrations [63]. This is attributed to low drug distribution and susceptibility to resistance mechanisms such as efflux transporters [30]. For this purpose, high doses of chemotherapeutic agents are administered to patients which causes high systemic toxicity. Therefore, enhancing the cytotoxic effect of administered chemotherapeutic agent decreases the required

Table 3 IC₅₀ of Pure GEF, GEF-NLC, and GEF-TPGS-NLC on Cell Viability of A549 Cell Line Using MTT Assay After 24 h and 48 h

Duration	Pure GEF	GEF-NLC	GEF-TPGS-NLC
24 h	11.16	15.05	7.01
48 h	3.54	4.35	3.60

GEF gefitinib, GEF-NLC gefitinib-loaded- nanostructural lipid carrier, GEF-TPGS-NLC gefitinib-loaded PEGylated nanostructural lipid carrier

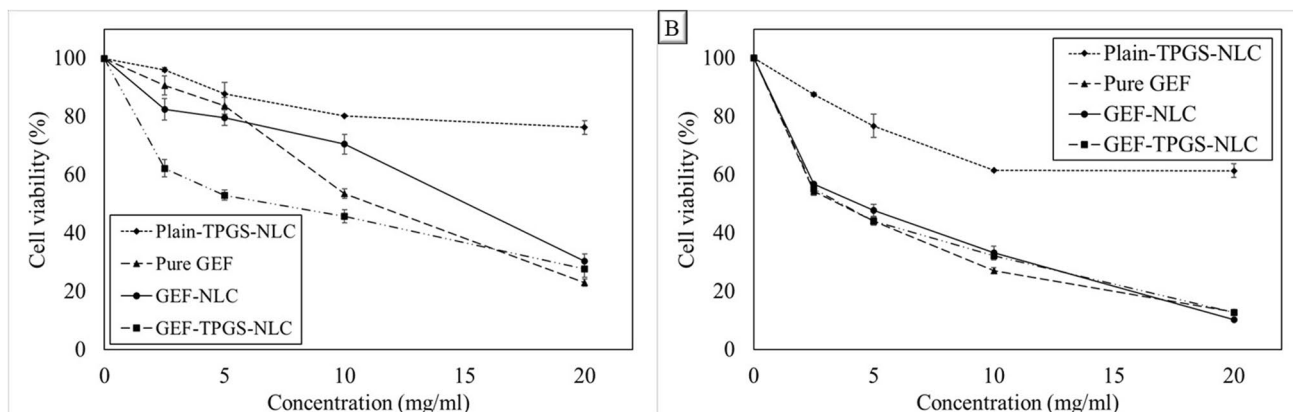
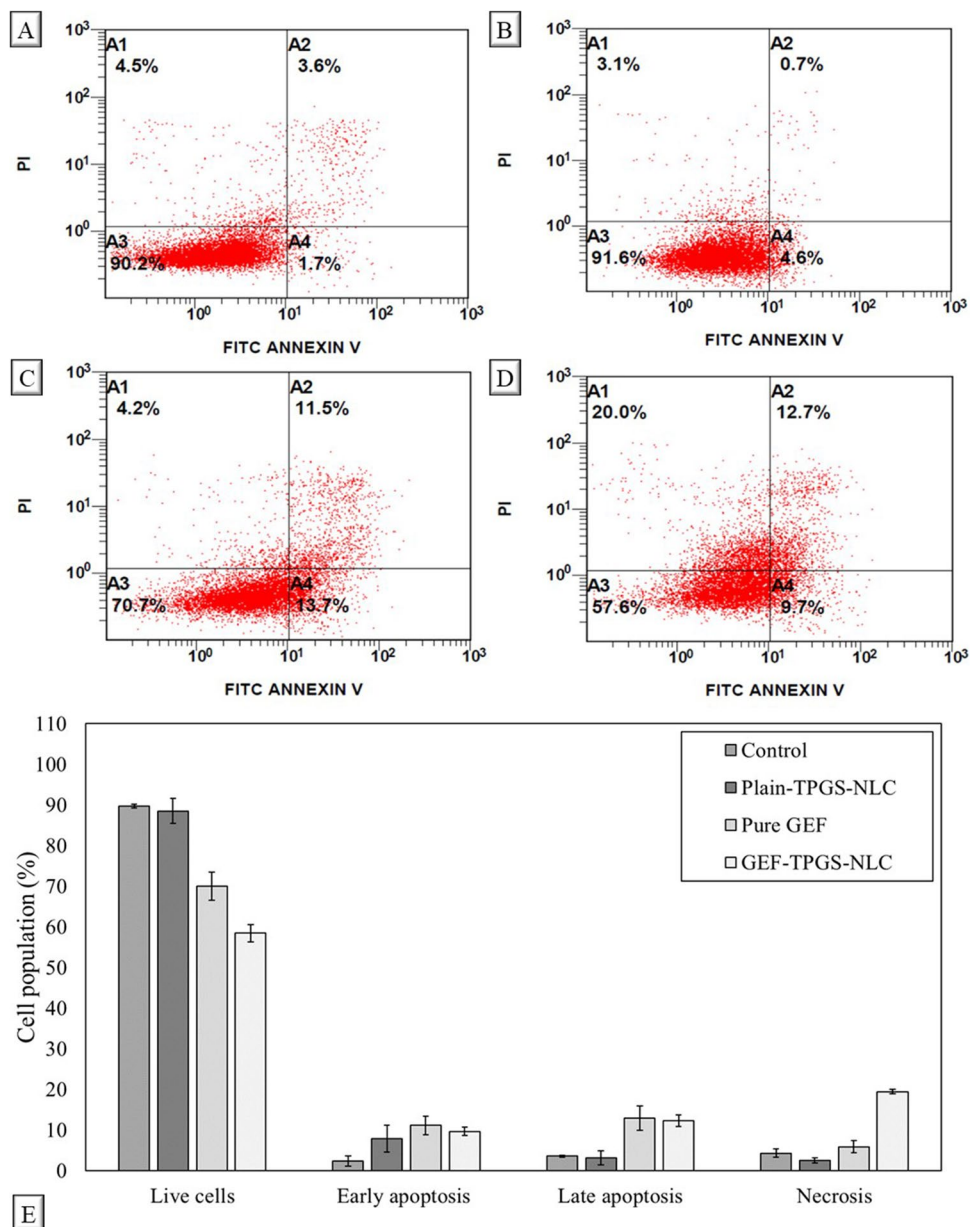


Fig. 8 Effect of pure GEF, Plain-TPGS-NLC, GEF-NLC, and GEF-TPGS-NLC on cell viability of A549 cell line using MTT assay treated with different concentrations (2.5, 5, 10, and 20 µg/mL) after **A** 24 h and **B** 48 h. Data were expressed as the mean ± SD, N=3

Fig. 9 Flow cytometric analysis of A549 cell line treated with **A** control, **B** Plain-TPGSNLC, **C** pure GEF, and **D** GEF-TPGS-NLC at 11.15 $\mu\text{g/ml}$ concentration. (A1, A2, A3, and A4) Necrotic, late apoptotic, early apoptotic, and viable cells are shown in the upper left quadrant, upper right quadrant, lower right quadrant, and lower left quadrant, respectively. **E** Bar chart shows the percentage of live, early apoptosis, late apoptosis, and necrotic cells that were treated with control, Plain-TPGS-SLN, pure GEF, and GEF-TPGS-SLN. Data were expressed as the mean \pm SD, $N=3$, p -value significant at *0.05, **0.01, and ***0.001. Plain-TPGS-NLC, drug-free engineered TPGS nanostructural lipid carrier; GEF-TPGS-NLC, gefitinib-loaded engineered TPGS nanostructural lipid carrier



therapeutic response besides low side effects [37]. Along with, encapsulation of therapeutic agents within an appropriate lipoprotein mimic carrier enhances cellular uptake and lung biodistribution [64]. This prevents GEF from binding to plasma proteins which increase the percentage of a free drug for biodistribution [30]. Therefore, the developed GEF-TPGS-NLC enhances the cytotoxic activity of GEF at lower concentrations. This might improve the therapeutic outcomes of GEF during in vivo administration.

In agreement with the obtained results, Hu et al. found that GEF-loaded lipid-based nanoformulation was able to enhance the apoptotic activity of GEF. The results revealed that the GEF-loaded formulation was able to increase the apoptotic cells population of A549 when compared with

pure GEF [22]. In addition, Pang et al. developed GEF-loaded albumin nanoparticles which it was able to induce apoptosis in treated cells when compared with pure GEF [39]. Furthermore, Wang et al. prepared SLN consisting of SA for the treatment of lung cancer. The biodistribution study showed that higher drug concentration was detected in lung tissue [64]. In addition, the presence of TPGS in the case of GEF-TPGS-NLC resulted in a significant enhancement in the bioactivity of GEF. This is achieved through drug internalization and efflux inhibitory effect [56]. This ensured the presence of a cytotoxic agent inside the cell instead outside. Therefore, it could be concluded that GEF-P-NLC produces cytotoxic activity through the aforementioned mechanism. This not only increases the efficacy of

therapeutic outcomes but also decreases the toxicity of GEF by decreasing the required dose [49]. Taken all together, TPGS engineered nanoscale lipid-based LDDS is expected to increase the therapeutic outcomes of GEF during the treatment of metastatic lung cancer.

Conclusion

In the present study, the nanoscale lipid-based formulations GEF-SLN, GEF-NLC, and GEF-LE were successfully prepared and physicochemically characterized. The plain formulations were smaller than GEF-loaded formulations. However, increasing lipid concentration resulted in decreased particle size of GEF-loaded formulation. GEF-NLC contained a high amount of lipid and showed a sustained drug release. The optimized GEF-NLC formulation was coated with TPGS and showed a slight increase in the particle size with a slight reduction in drug release. Cytotoxicity showed that IC_{50} of pure GEF was 11.15 $\mu\text{g/ml}$ which decreased to 7.05 for GEF-TPGS-NLC. Moreover, the cytotoxicity studies revealed that TPGS engineered NLC decreased the number of living cells compared to pure GEF. The obtained results indicated that TPGS engineered NLC are pretended to improve the therapeutic impact of GEF in the treatment of metastatic lung cancer. Further in vivo studies are required to address this issue.

Author Contribution Conceptualization, Data curation, visualization, and Formal analysis, A.Y. S. and G. I. H.; Funding acquisition, F.K. A.; Investigation, A.Y. S. and G. I. H.; Methodology, A.Y. S., G. I. H., F.A.N., and A.S.A.; Project administration, F.K. A. Resources, A.Y. S. and G. I. H.; Software, A.Y. S. and G. I. H.; Supervision, F.K. A. and G. I. H.; Validation, A.Y. S.; Writing (original draft), A.Y. S. and G. I. H.; Writing (review and editing), F.K. A. and G. I. H.

Funding The authors extend their appreciation to the Deanship of Scientific Research, King Saud University for funding through Vice Deanship of Scientific Research Chairs, Kayyali Chair for Pharmaceutical Industry, Department of Pharmaceutics, College of Pharmacy, for funding the work through Grant Number AG-2022-3.

Declarations

Conflict of Interest The authors declare no competing interests.

References

- Abdellatif A, Abou-Taleb HA. Optimization of nano-emulsion formulations for certain emollient effects. *J Pharm Pharm Sci*. 2015;4:1314–28.
- Aditya N, Macedo AS, Doktorovova S, Souto EB, Kim S, Chang P-S, Ko S. Development and evaluation of lipid nanocarriers for quercetin delivery: a comparative study of solid lipid nanoparticles (SLN), nanostructured lipid carriers (NLC), and lipid nanoemulsions (LNE). *LWT-Food Science and Technology*. 2014;59:115–21.
- Alajami HN, Fouad EA, Ashour AE, Kumar A, Yassin AEB. Celecoxib-loaded solid lipid nanoparticles for colon delivery: formulation optimization and in vitro assessment of anti-cancer activity. *Pharmaceutics*. 2022;14:131.
- Alshehri S, Alanazi A, Elzayat EM, Altamimi MA, Imam SS, Hussain A, Alqahtani F, Shakeel F. Formulation, in vitro and in vivo evaluation of gefitinib solid dispersions prepared using different techniques. *Processes*. 2021;9:1210.
- Baek J-S, Cho C-W. Surface modification of solid lipid nanoparticles for oral delivery of curcumin: improvement of bioavailability through enhanced cellular uptake, and lymphatic uptake. *Eur J Pharm Biopharm*. 2017;117:132–40.
- Bagheri A, Moezzi SMI, Mosaddeghi P, Parashkouhi SN, Hoseini SMF, Badakhshan F, Negahdaripour M. Interferon-inducer antivirals: potential candidates to combat COVID-19. *Int Immunopharmacol*. 2021;91: 107245.
- Banerjee P, Geng T, Mahanty A, Li T, Zong L, Wang B. Integrating the drug, disulfiram into the vitamin E-TPGS-modified PEGylated nanostructured lipid carriers to synergize its repurposing for anti-cancer therapy of solid tumors. *Int J Pharm*. 2019;557:374–89.
- Barba AA, Bochicchio S, Dalmoro A, Caccavo D, Cascone S, Lamberti G. Polymeric and lipid-based systems for controlled drug release: an engineering point of view. *Nanomaterials for drug delivery and therapy*: Elsevier; 2019.
- Cho H-J, Park JW, Yoon I-S, Kim D-D. Surface-modified solid lipid nanoparticles for oral delivery of docetaxel: enhanced intestinal absorption and lymphatic uptake. *Int J Nanomed*. 2014;9:495.
- Danaei M, Dehghankhold M, Ateei S, Hasanazadeh Davarani F, Javanmard R, Dokhani A, Khorasani S, Mozafari M. Impact of particle size and polydispersity index on the clinical applications of lipidic nanocarrier systems. *Pharmaceutics*. 2018;10:57.
- Dandekar PP, Jain R, Patil S, Dhupal R, Tiwari D, Sharma S, Vanage G, Patravale V. Curcumin-loaded hydrogel nanoparticles: application in anti-malarial therapy and toxicological evaluation. *J Pharm Sci*. 2010;99:4992–5010.
- Dantas IL, Bastos KTS, Machado M, Galvão JG, Lima AD, Gonçalves JKMC, Almeida EDP, Araújo AAS, de Menezes CT, Sarmiento VHV. Influence of stearic acid and beeswax as solid lipid matrix of lipid nanoparticles containing tacrolimus. *J Therm Anal Calorim*. 2018;132:1557–66.
- Das SS, Alkahtani S, Bharadwaj P, Ansari MT, Alkahtani MD, Pang Z, Hasnain MS, Nayak AK, Aminabhavi T. Molecular insights and novel approaches for targeting tumor metastasis. *Int J Pharmaceutics*. 2020;119556.
- Dumont C, Bourgeois S, Fessi H, Jannin V. Lipid-based nano-suspensions for oral delivery of peptides, a critical review. *Int J Pharm*. 2018;541:117–35.
- Fathy M, El-Badry M. Preparation and evaluation of piroxicam-pluronic solid dispersions. *Bulletin of Pharmaceutical Sciences Assiut*. 2003;26:97–108.
- Ganta S, Amiji M. Coadministration of paclitaxel and curcumin in nanoemulsion formulations to overcome multidrug resistance in tumor cells. *Mol Pharm*. 2009;6:928–39.
- Godugu C, Doddapaneni R, Patel AR, Singh R, Mercer R, Singh M. Novel gefitinib formulation with improved oral bio-availability in treatment of A431 skin carcinoma. *Pharm Res*. 2016;33:137–54.
- Harisa GI, Alomrani AH, Badran MM. Simvastatin-loaded nanostructured lipid carriers attenuate the atherogenic risk of erythrocytes in hyperlipidemic rats. *Eur J Pharm Sci*. 2017;96:62–71.
- Harisa GI, Badran MM. Simvastatin nanolipid carriers decreased hypercholesterolemia induced cholesterol inclusion and

- phosphatidylserine exposure on human erythrocytes. *J Mol Liq.* 2015;208:202–10.
20. Harisa GI, Sherif AY, Youssof AM, Alanazi FK, Salem-Bekhit MM. Bacteriosomes as a promising tool in biomedical applications: immunotherapy and drug delivery. *AAPS PharmSciTech.* 2020;21:1–13.
 21. He R, Zang J, Zhao Y, Dong H, Li Y. Nanotechnology-based approaches to promote lymph node targeted delivery of cancer vaccines. *ACS Biomater Sci Eng.* 2022;8:406–23.
 22. Hu Y, Zhang J, Hu H, Xu S, Xu L, Chen E. Gefitinib encapsulation based on nano-liposomes for enhancing the curative effect of lung cancer. *Cell Cycle.* 2020;19:3581–94.
 23. Huang Y, Nan L, Xiao C, Ji Q, Li K, Wei Q, Liu Y, Bao G. Optimum preparation method for self-assembled pegylation nano-adjuvant based on *Rehmannia glutinosa* polysaccharide and its immunological effect on macrophages. *Int J Nanomed.* 2019;14:9361.
 24. Iqbal B, Ali J, Baboota S. Silymarin loaded nanostructured lipid carrier: from design and dermatokinetic study to mechanistic analysis of epidermal drug deposition enhancement. *J Mol Liq.* 2018;255:513–29.
 25. Jain A, Sharma G, Thakur K, Raza K, Shivhare U, Ghoshal G, Katare OP. Beta-carotene-encapsulated solid lipid nanoparticles (BC-SLNs) as promising vehicle for cancer: an investigative assessment. *AAPS PharmSciTech.* 2019;20:1–7.
 26. Koban R, Neumann M, Nelson PP, Ellerbrok H. Differential efficacy of novel antiviral substances in 3D and monolayer cell culture. *Viruses.* 2020;12:1294.
 27. Li J, Yang M, Xu W. Development of novel rosuvastatin nanostructured lipid carriers for oral delivery in an animal model. *Drug Des Dev Ther.* 2018;12:2241.
 28. Liu G, Lin Q, Huang Y, Guan G, Jiang Y. Tailoring the particle microstructures of gefitinib by supercritical CO₂ anti-solvent process. *J CO₂ Utilization.* 2017;20:43–51.
 29. Luiz MT, di Filippo LD, Alves RC, Araújo VHS, Duarte JL, Marchetti JM, Chorilli M. The use of TPGS in drug delivery systems to overcome biological barriers. *Eur Polymer J.* 2021;142:110129.
 30. Makeen HA, Mohan S, Al-Kasim MA, Attafi IM, Ahmed RA, Syed NK, Sultan MH, Al-Bratty M, Alhazmi HA, Safhi MM. Gefitinib loaded nanostructured lipid carriers: characterization, evaluation and anti-human colon cancer activity in vitro. *Drug Delivery.* 2020;27:622–31.
 31. Mehmood T, Ahmad A, Ahmed A, Ahmed Z. Optimization of olive oil based O/W nanoemulsions prepared through ultrasonic homogenization: a response surface methodology approach. *Food Chem.* 2017;229:790–6.
 32. Mitchell MJ, Billingsley MM, Haley RM, Wechsler ME, Peppas NA, Langer R. Engineering precision nanoparticles for drug delivery. *Nat Rev Drug Discovery.* 2021;20:101–24.
 33. Moghimi SM, Szebeni J. Stealth liposomes and long circulating nanoparticles: critical issues in pharmacokinetics, opsonization and protein-binding properties. *Prog Lipid Res.* 2003;42:463–78.
 34. Nakamura T, Harashima H. Dawn of lipid nanoparticles in lymph node targeting: potential in cancer immunotherapy. *Adv Drug Deliv Rev.* 2020;167:78–88.
 35. Nasr FA, Noman OM, Alqahtani AS, Qamar W, Ahamad SR, Al-Mishari AA, Alyhya N, Farooq M. Phytochemical constituents and anticancer activities of *Tarhomonanthus camphoratus* essential oils grown in Saudi Arabia. *Saudi Pharmaceutical Journal.* 2020;80:1474–80.
 36. Nayek S, Raghavendra N, Kumar BS. Development of novel S PC-3 gefitinib lipid nanoparticles for effective drug delivery in breast cancer. Tissue distribution studies and cell cytotoxicity analysis. *J Drug Delivery Sci Technol.* 2020;102073.
 37. Nayek S, Raghavendra N, Kumar BS. Development of novel S PC-3 gefitinib lipid nanoparticles for effective drug delivery in breast cancer. Tissue distribution studies and cell cytotoxicity analysis. *J Drug Delivery Sci Technol.* 2021;61:102073.
 38. Noor, R. 2021. Developmental status of the potential vaccines for the mitigation of the COVID-19 Pandemic and a focus on the effectiveness of the Pfizer-BioNTech and Moderna mRNA vaccines. *Current clinical microbiology reports,* 8, 178-185.
 39. Pang X, Yang P, Wang L, Cao J, Cheng Y, Sheng D, Wan X, Guo Q, Qian K, Zhang Q. Human serum albumin nanoparticulate system with encapsulation of gefitinib for enhanced anti-tumor effects in non-small cell lung cancer. *Journal of Drug Delivery Science and Technology.* 2019;52:997–1007.
 40. Paranjpe M, Finke J, Richter C, Gothsch T, Kwade A, Büttgenbach S, Müller-Goymann C. Physicochemical characterization of sildenafil-loaded solid lipid nanoparticle dispersions (SLN) for pulmonary application. *Int J Pharm.* 2014;476:41–9.
 41. Patel P, Patel M. Enhanced oral bioavailability of nintedanib esylate with nanostructured lipid carriers by lymphatic targeting: In vitro, cell line and in vivo evaluation. *Eur J Pharm Sci.* 2021;159: 105715.
 42. Pawar AA, Chen D-R, Venkataraman C. Influence of precursor solvent properties on matrix crystallinity and drug release rates from nanoparticle aerosol lipid matrices. *Int J Pharm.* 2012;430:228–37.
 43. Permana AD, Nainu F, Moffatt K, Larrañeta E, Donnelly RF. Recent advances in combination of microneedles and nanomedicines for lymphatic targeted drug delivery. *Wiley Interdisciplinary Reviews: Nanomedicine and Nanobiotechnology.* 2021;13: e1690.
 44. Pilkington EH, Suys EJ, Trevaskis NL, Wheatley AK, Zukanic D, Algarni A, Al-Wassiti H, Davis TP, Pouton CW, Kent SJ. From influenza to COVID-19: lipid nanoparticle mRNA vaccines at the frontiers of infectious diseases. *Acta Biomater.* 2021;131:16–40.
 45. Qarmout, M. Y. A. 2021. Use of lymphatic systems for absorption of nano-particles. *Asian Journal of Pharmaceutics (AJP): Free full text articles from Asian J Pharm,* 15.
 46. Raj SB, Chandrasekhar KB, Reddy KB. Formulation, in-vitro and in-vivo pharmacokinetic evaluation of simvastatin nanostructured lipid carrier loaded transdermal drug delivery system. *Future Journal of Pharmaceutical Sciences.* 2019;5:1–14.
 47. Rigon RB, González ML, Severino P, Alves DA, Santana MH, Souto EB, Chorilli M. Solid lipid nanoparticles optimized by 22 factorial design for skin administration: cytotoxicity in NIH3T3 fibroblasts. *Colloids Surf, B.* 2018;171:501–5.
 48. Shao J, Xu Z, Peng X, Chen M, Zhu Y, Xu L, Zhu H, Yang B, Luo P, He Q. Gefitinib synergizes with irinotecan to suppress hepatocellular carcinoma via antagonizing Rad51-mediated DNA-repair. *PLoS ONE.* 2016;11: e0146968.
 49. Sherif AY, Harisa GI, Alanazi FK, Youssof AM. Engineering of exosomes: steps towards green production of drug delivery system. *Curr Drug Targets.* 2019;20:1537–49.
 50. Shinde UA, Parmar SJ, Easwaran S. Metronidazole-loaded nanostructured lipid carriers to improve skin deposition and retention in the treatment of rosacea. *Drug Dev Ind Pharm.* 2019;45:1039–51.
 51. Shirazi AS, Varshochian R, Rezaei M, Ardakani YH, Dinarvand R. SN38 loaded nanostructured lipid carriers (NLCs); preparation and in vitro evaluations against glioblastoma. *J Mater Sci - Mater Med.* 2021;32:1–12.
 52. Singh H, Gupta R, Gautam G. Formulation development, characterization, and in vitro-in vivo study of antihyperlipidemic drug rosuvastatin calcium—solid lipid nanoparticles. *Asian J Pharm Clin Res.* 2018;11:436–43.

53. Skinner O, Boston S, Giglio R, Whitley E, Colee J, Porter E. Diagnostic accuracy of contrast-enhanced computed tomography for assessment of mandibular and medial retropharyngeal lymph node metastasis in dogs with oral and nasal cancer. *Veterinary and comparative oncology*. 2018;16:562–70.
54. Srinivas NSK, Verma R, Kulyadi GP, Kumar L. A quality by design approach on polymeric nanocarrier delivery of gefitinib: formulation, in vitro, and in vivo characterization. *Int J Nanomed*. 2017;12:15.
55. Swidan SA, Mansour ZN, Mourad ZA, Elhesaisy NA, Mohamed NA, Bekheet MS, Badawy MA, Elsemeiri MM, Elrefaey AE, Hasaneen AM. DOE, formulation, and optimization of repaglinide nanostructured lipid carriers. *JAPS*. 2018;8:8–16.
56. Tong M, Wu X, Zhang S, Hua D, Li S, Yu X, Wang J, Zhang Z. Application of TPGS as an efflux inhibitor and a plasticizer in baicalein solid dispersion. *Eur J Pharm Sci*. 2022;168: 106071.
57. Tortorici S, Cimino C, Ricupero M, Musumeci T, Biondi A, Siscaro G, Carbone C, Zappalà L. Nanostructured lipid carriers of essential oils as potential tools for the sustainable control of insect pests. *Ind Crops Prod*. 2022;181: 114766.
58. Tsai H-I, Jiang L, Zeng X, Chen H, Li Z, Cheng W, Zhang J, Pan J, Wan D, Gao L. DACHPt-loaded nanoparticles self-assembled from biodegradable dendritic copolymer polyglutamic acid-bD- α -tocopheryl polyethylene glycol 1000 succinate for multidrug resistant lung cancer therapy. *Front Pharmacol*. 2018;9:119.
59. Vaidya A, Jain S, Jain A, Jain A. Simvastatin-loaded PEGylated solid lipid nanoparticles: lipid functionalization to improve blood circulation. *Bionanoscience*. 2020;10:773–82.
60. Vandghanooni S, Rasouljan F, Eskandani M, AKBARI NAKH-JAVANI, S. & ESKANDANI, M. Acriflavine-loaded solid lipid nanoparticles: preparation, physicochemical characterization, and anti-proliferative properties. *Pharm Dev Technol*. 2021;26:934–42.
61. Vishwakarma N, Jain A, Sharma R, Mody N, Vyas S, Vyas SP. Lipid-based nanocarriers for lymphatic transportation. *AAPS PharmSciTech*. 2019;20:1–13.
62. Wang C, Cui C. Inhibition of lung cancer proliferation by wogonin is associated with activation of apoptosis and generation of reactive oxygen species. *Balkan Med J*. 2020;37:29.
63. Wang J, Wang F, Li X, Zhou Y, Wang H, Zhang Y. Uniform carboxymethyl chitosan-enveloped Pluronic F68/poly (lactic-co-glycolic acid) nano-vehicles for facilitated oral delivery of gefitinib, a poorly soluble antitumor compound. *Colloids Surf, B*. 2019;177:425–32.
64. Wang P, Zhang L, Peng H, Li Y, Xiong J, Xu Z. The formulation and delivery of curcumin with solid lipid nanoparticles for the treatment of on non-small cell lung cancer both in vitro and in vivo. *Mater Sci Eng, C*. 2013;33:4802–8.
65. Wang X, Qiu Y, Wang M, Zhang C, Zhang T, Zhou H, Zhao W, Zhao W, Xia G, Shao R. Endocytosis and organelle targeting of nanomedicines in cancer therapy. *Int J Nanomed*. 2020;15:9447.
66. YANG, Y., CORONA III, A., SCHUBERT, B., REEDER, R. & HENSON, M. A. The effect of oil type on the aggregation stability of nanostructured lipid carriers. *J Colloid Interface Sci*. 2014;418:261–72.
67. Ye F, Zhang D, Xu X, Guo H, Liu S, Zhang S, Wu Y, Zhu W-H. Anchorable perylene diimides as chemically inert electron transport layer for efficient and stable perovskite solar cells with high reproducibility. *Solar RRL*. 2021;5:2000736.
68. Zardini AA, Mohebbi M, Farhoosh R, Bolurian S. Production and characterization of nanostructured lipid carriers and solid lipid nanoparticles containing lycopene for food fortification. *J Food Sci Technol*. 2018;55:287–98.
69. Zarrintaj P, Ramsey JD, Samadi A, Atoufi Z, Yazdi MK, Ganjali MR, Amirabad LM, Zangene E, Farokhi M, Formela K. Poloxamer: a versatile tri-block copolymer for biomedical applications. *Acta Biomater*. 2020;110:37–67.
70. Zhang X-Y, Lu W-Y. Recent advances in lymphatic targeted drug delivery system for tumor metastasis. *Cancer Biol Med*. 2014;11:247.
71. Zhang Y, Zhang P, Zhu T. Ovarian carcinoma biological nanotherapy: comparison of the advantages and drawbacks of lipid, polymeric, and hybrid nanoparticles for cisplatin delivery. *Biomed Pharmacother*. 2019;109:475–83.
72. Zhao X, Sun Y, Li Z. Topical anesthesia therapy using lidocaine-loaded nanostructured lipid carriers: tocopheryl polyethylene glycol 1000 succinate-modified transdermal delivery system. *Drug Des Dev Ther*. 2018;12:4231.

Publisher's Note Springer Nature remains neutral with regard to jurisdictional claims in published maps and institutional affiliations.